

REFORMER MODEL DEVELOPMENT FOR HYDROGEN PRODUCTION

J. Bellan*, N. Okong'o, P. C. LeClercq and H. Abdel-Hameed
Jet Propulsion Laboratory
California Institute of Technology
4800 Oak Grove Drive
*MS. 125-109
Pasadena, California 91109-8099
*Tel: (818) 354-6959, *Fax: (818) 393-5011
josette.bellan@jpl.nasa.gov

The long-term goal of this investigation is the quantitative prediction of the hydrogen yield from drops of an evaporating diesel fuel spray in steam, leading to an optimization study for maximizing the hydrogen yield and scale-up to commercial reactors.

The physical configuration is as follows: a spray of diesel fuel is injected into a chamber containing water steam, the fuel drops evaporate and the evaporated species reacts with the steam (steam reforming) to yield hydrogen and carbon dioxide. The generic, global chemical reaction is $C_nH_m + 2nH_2O \rightarrow nCO_2 + (0.5m + 2n)H_2$, and the interest is in maximizing the hydrogen yield. This is a modeling and computational approach, as numerical simulations provide a financially economic way of process optimization and scale-up when considering the influence of many parameters.

To ensure that the model is quantitative, two elements are necessary, as follows:

- (1) an appropriate spray model combining the turbulent behavior of drops and gas with the evaporative process, and
- (2) an appropriate reaction scheme and kinetic parameters portraying reforming.

The focus of this year's activities is on the spray dynamics and evaporation. Three different topics are addressed, all of them in the framework of Direct Numerical Simulations (DNS). DNS are deterministic simulations wherein all scales of the flow are resolved, albeit for a domain much smaller than that of interest (due to the computational necessity of resolving all scales of turbulence – e.g. about 10^8 in each of the 3 directions – even for gaseous flows). These DNS are very computational intensive calculations whose sole purpose is the extraction of Subgrid Scale (SGS) models, which embed the essence of turbulence. These SGS models are meant to be used in Large Eddy Simulations (LES), which are considerably less computationally intensive than DNS (by orders of magnitude). The equations solved in LES are obtained by filtering the DNS conservation equations so as to remove the small scales. Thus, in LES only the large scales of the flow are resolved and the small scales must be modeled (by the SGS).

In DNS, the computational goal is the achievement of a transitional state (not fully turbulent, but having reached the threshold to turbulence), which serves as a basis for the extraction of SGS models. Credible SGS models for drop-laden flows with evaporation are not currently available. Therefore, the goals of the current study are to:

- (i) create a database from which to extract (SGS) models for further use in (LES) of turbulent sprays,
- (ii) evaluate, in the laminar context, the ability of sprays with different cross-section injection geometry to disperse the drops and mix the evaporated species with the surrounding gas, so as to improve the reaction effectiveness, and

(iii) develop a model allowing the determination of the differences in results (if any) between relatively less expensive simulations with a single-component hydrocarbon used to portray a complex hydrocarbon mixture (i.e. diesel fuel), and more expensive simulations using a model for the mixture.

DIRECT NUMERICAL SIMULATIONS CONSISTENT WITH LARGE EDDY SIMULATIONS

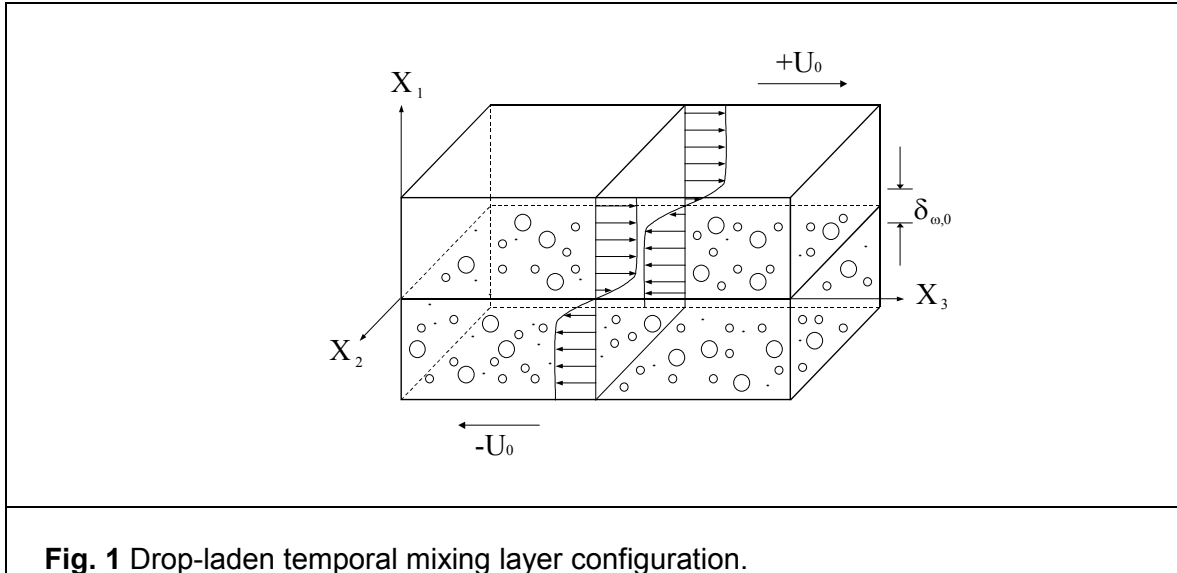
The utilization of SGS derived models from DNS into LES is based on the combined assumptions of small (i.e. Kolmogorov) scale isotropy and similarity of SGS dependency on the resolved scale (i.e. LES) variables for transitional and fully turbulent regimes. These assumptions are inherent in the DNS/LES approach, but neither one of them is entirely established for gaseous, let alone general drop-laden flows. The small-scale isotropy is, in particular, dependent on the ratio of the Kolmogorov scale (the smallest turbulence scale) to the drop diameter. In this study, the drops being much smaller than the Kolmogorov scale, the issue of small-scale isotropy reduces to that for gaseous flows. The similarity of transitional and fully turbulent regime SGS dependency on the resolved scale variables is an issue that should be confronted in future comparisons between results from LES utilizing DNS-derived SGS models and equivalent experimental data.

However, a more pervasive assumption is also typically made in DNS of particle-laden flows targeting high temperature applications: the neglect of the diffusion velocity contribution in the heat flux, emulating some modeling of flows with combustion. This assumption is not inherent in the DNS/LES approach, and can be evaluated using a DNS database. This evaluation is particularly important for DNS consistency since the initial gas temperature is chosen relatively low in DNS to insure that the drops survive long enough to interact with the flow. A posteriori analysis of our previous databases excluding the diffusion velocity contribution revealed that at these low gas temperatures, the diffusion velocity term magnitude rivals and sometimes exceeds the heat conduction term. Admittedly, this does not constitute proof of the importance of these terms because they were not included in the energy equation corresponding to the database; however, this is an indication that the assumption should be re-evaluated.

In principle, any SGS model derived from a DNS is physically correct only if this diffusion velocity term is included. This is true even if the SGS model is intended for use under high gas-temperature conditions. Basically, the DNS equations should be self consistent for the conditions of the DNS regime, and the projected applicability of DNS derived results to fully developed turbulent flow should be left as a hypothesis standing on its own, and unburdened by other assumptions.

To obtain new databases (representing transitional states) including the diffusion velocity contribution to the heat flux, a new set of simulations was here conducted by including this term in the energy equation of our previous studies. The configuration is displayed in Fig. 1 and depicts a temporal mixing layer; a spatial mixing layer is too computationally intensive to be amenable to DNS. Figure 1 depicts two countercurrent streams, the lower one being initially laden with drops. The computations are started with 4 vortices in the streamwise (i.e. x_1) and spanwise (i.e. x_3) directions, and the layer is perturbed to initiate entrainment of the drops and gas, and pairing of the initial vortices into an ultimate vortex in which small, turbulent scales proliferate. The attainment of transition is based on the examination of global layer quantities which are manifestations of growth, small-scale induced vorticity, flow stretching and tilting effects, which are inherent to turbulence, and finally on the energy spectra based on velocity fluctuations; at transition, these energy spectra display a smooth aspect typical of turbulence.

Transitional states have been obtained for several simulations, including simulations with and without drops, all of which are listed in Table 1. The Stokes number (St), whose initial value is listed in Table 1, is a measure of the degree of interaction of the drops with the flow: for $St < 1$, the drops follow the flow, for $St > 1$, the drops assume a 'ballistic' behavior, whereas for $St \approx 1$, the drops tend to accumulate at the periphery of vortices. This accumulation is evident, as an example, in Fig. 2 displaying the drop number density for run TP500b at the transitional state in the $x_3 = 0.06m$ (the between-the-braid) plane.



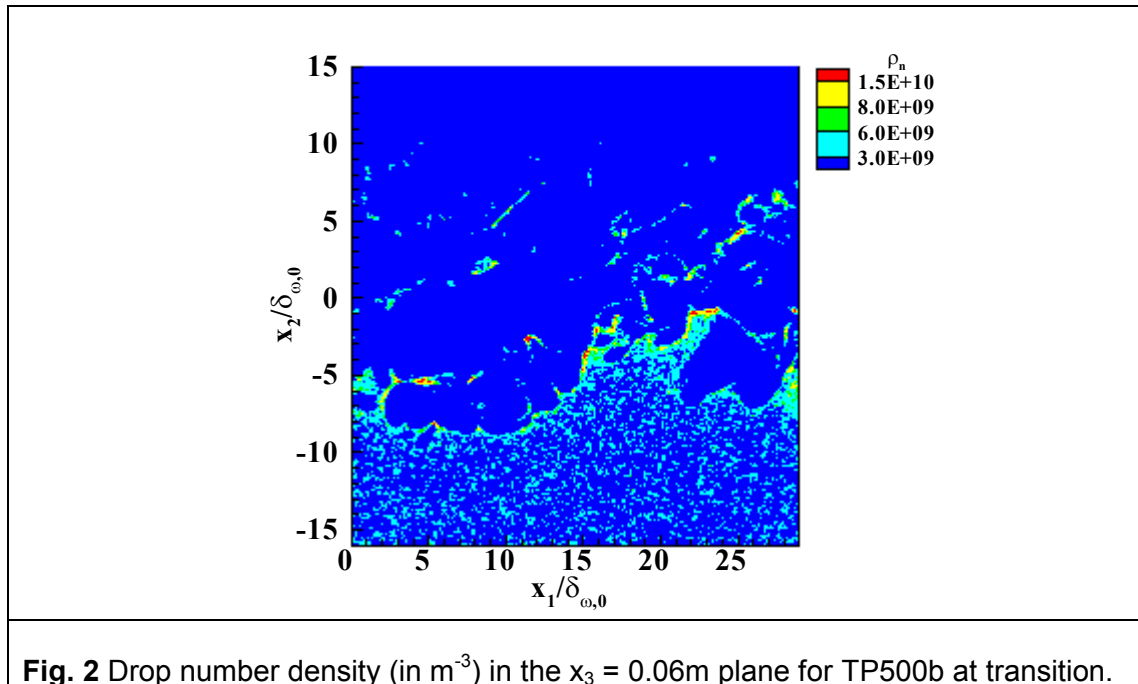
Run	Re_0	ML_0	St_0 distribution: mean \pm variance	Number of drops	Resolution (number of points)	$Re_{m,tr}$
SP500	500	0	0 ± 0	0	256 x 288 x 160	1290
SP600	500	0	0 ± 0	0	288 x 320 x 176	1491
TP500a	500	0.2	3.0 ± 0.5	2,277,222	256 x 288 x 160	1414
TP500b	500	0.5	3.0 ± 0.5	5,693,055	256 x 288 x 160	1361
TP500c	500	0.2	1.5 ± 0.5	6,440,956	256 x 288 x 160	1418
TP500d	500	0.2	3.0 ± 0.25	2,292,822	256 x 288 x 160	1411
TP600a	600	0.2	3.0 ± 0.5	2,993,630	288 x 320 x 176	1576
TP600b	600	0.5	3.0 ± 0.5	7,484,075	288 x 320 x 176	1676

Table 1. List of DNS conducted. Re_0 is the initial Reynolds number, ML_0 is the initial mass loading (drops/gas), and $Re_{m,tr}$ is the momentum-thickness-based Reynolds number at transition, where the momentum thickness measures the growth of the layer. All simulations were conducted on a SGI Origin 2000 supercomputer, using 64 processors. For all simulations, the liquid is n-decane and the domain size is 0.2m x 0.22m x 0.12m.

The databases created have been analyzed at different physical times including the final simulation time, and the budget of the energy equation has been evaluated in order to assess the validity of neglecting the diffusion velocity contribution. The results show that the neglect of

the diffusion velocity contribution is not a good assumption, as its contribution overwhelms that of the thermal conductivity in the heat flux.

The databases created above have been, and are still being analyzed. For example, the contributions of various physical mechanisms to the small-scale gaseous dissipation (which is the quantity that it is desirable to reproduce through SGS) were evaluated [1]. To undertake this study, we first derived the entropy equation for the gas in the context of a drop-laden gaseous flow.



The dissipation is in fact the irreversible entropy production, and it can be evaluated from the DNS database using the appropriate terms of the entropy equation developed herein. By calculating the filtered dissipation and taking the difference between the unfiltered and filtered values, one obtains the dissipation associated with the small scales of the flow. The irreversible entropy production generally contains gas-boundary-generated terms, viscous dissipation terms, heat dissipation terms and species (i.e. scalar) dissipation terms. The gas-boundary-generated terms are those associated with the source terms in the conservation equations, as each real (i.e. DNS) drop boundary constitutes a boundary for the gas phase. Indeed, each drop represents a source/sink for the gaseous flow: for the mass (due to evaporation), for momentum (due to drag and evaporation) and for energy (due to evaporation, drop heat up, kinetic energy of the evaporated gas and drag). With increasing mass loading, the contribution of these source terms becomes increasingly important. The results show that for drop-laden flow, the viscous dissipation, which is the only contributor to gaseous flows, is only the third contributor in magnitude to the dissipation, and about a factor of 5 to 7 smaller than the leading term. The two leading terms are the dissipation due to the energy of the mass entering the gas phase as a result of evaporation (which produces dissipation at the large scales, but removes dissipation at the small scales), and the dissipation due to the chemical potential term related to phase change (which removes dissipation at the large scales, but produces dissipation at the small

scales); these terms have never been modeled in the context of sprays, which may be one of the causes of current model failures to predict spray behavior.

It is noteworthy that in many gaseous flows the local dissipation is not well predicted by the SGS, especially if the model is of the Smagorinsky (SM) type. For example, a notorious situation falling in this category is the application of the constant-coefficient SM model to conditions where the strain rate and stress might not be locally aligned, such as in recirculating flows prevailing in sprays injected in enclosed chambers. In fact, the SM coefficient has been found to depend on the flow field, with different values for isotropic turbulence, channel flows and mixing layers. Although the lack of local correlation between some models and SGS fluxes is intellectually disturbing, in some gaseous flow LES calculations this deficiency may not be essential. In contrast, in drop-laden flows, because the source terms are locally produced, and because they may represent the highest small-scale dissipative contribution, the prediction of the local dissipation may become a very important goal. This constitutes one of the interests of our current work. We note that there is already evidence that LES results are highly dependent on the modeling of the source terms. For example, some investigators must assume that drops below an arbitrary size must instantaneously evaporate in order to obtain agreement between simulations and data [2]; such an assumption is ad-hoc because this threshold drop size will change with the flow geometry and other conditions. Despite this LES sensitivity to the source term model, the modeling of the source terms in the context of LES has never been addressed from first principles. This may be, however, of crucial importance to the reforming of the evaporated hydrocarbons because it is precisely the evaporated fuel that will be participating in the reforming reactions. The database is currently being analyzed to extract these models.

EFFECT OF DIFFERENT CROSS-SECTION SPRAY-INJECTION GEOMETRIES

In parallel with DNS of transitional mixing layers, and foreseeing the ultimate goal of optimizing hydrogen production from diesel spray reforming, we have investigated several cross-section injection geometries (circular, square, rectangular, ellipsoidal and triangular) for spatial drop-laden gaseous jets to determine if there is a particular geometry that is more beneficial to drop dispersion and mixing of the evaporated species with the gaseous surroundings. An example of such geometry is shown in Fig. 3 for a rectangular jet. For gaseous jets, there is already experimental as well as numerical evidence that jets with non-circular inlet geometries display superior entrainment and mixing characteristics [3] – [6]. However, there are no equivalent studies for drop-laden jets, i.e. sprays.

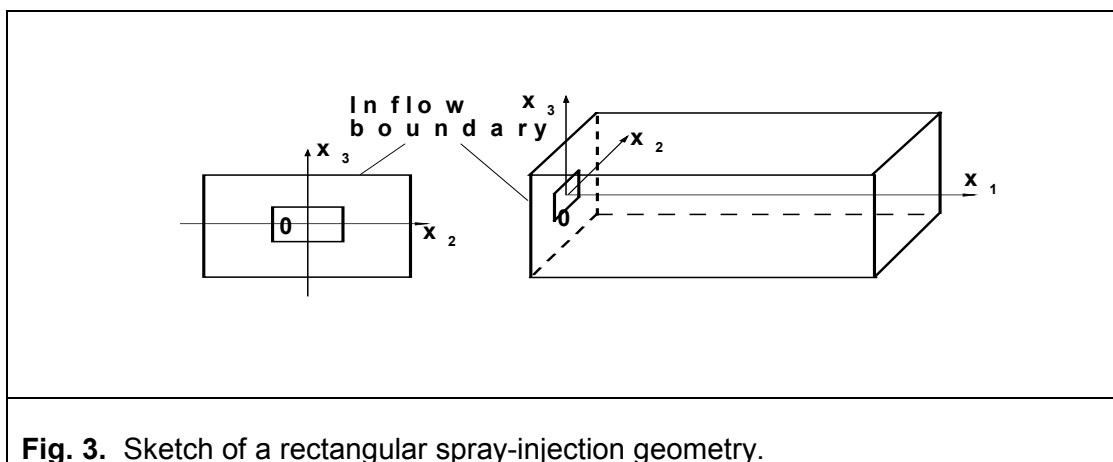


Fig. 3. Sketch of a rectangular spray-injection geometry.

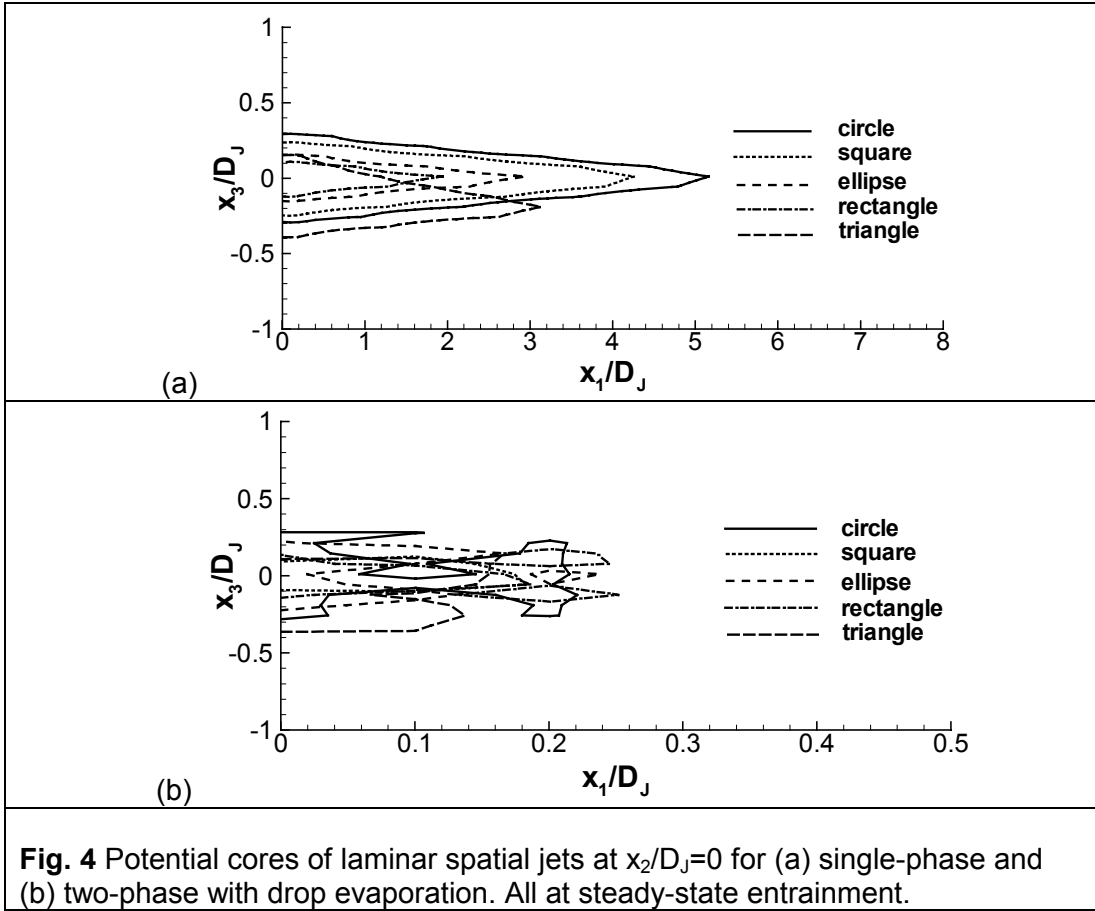
Therefore, we have conducted a DNS investigation in the context of laminar sprays to determine if the advantages observed for gaseous jets are translatable to evaporating sprays. The computational domain dimensions are $L_1 = 2L_2 = 2L_3 = 8D_J = 0.16\text{m}$. The boundaries of the domain in Fig. 3 are computational, as the jet is unconfined (free jet). The equivalent jet diameter D_J (which is the diameter of the circle that has the same area as the non-circular inlet sections) is chosen to be 0.02m for all geometric configurations; this means that while the cross-section geometry changes, the area is the same in all simulations. The elliptic configuration is chosen so that the major axis is in the x_2 direction, symmetrically centered about $x_3 = 0$ and with major and minor axis lengths of 0.028m and 0.014m, respectively. The square configuration is centered at $x_2 = x_3 = 0$ with sides of 0.0177m in length. The rectangle is also centered at $x_2 = x_3 = 0$ and has its larger side of length 0.025m along the x_2 axis, while its smaller side is 0.0125m in length. Finally, the triangle is equilateral, with a peak located at $x_2 = 0$ and $x_3 = 0.01166\text{m}$.

Specifically, for each of the above-stated geometries, we conducted simulations for spatial, both gaseous and drop-laden jets and compared the results (i) between gaseous and drop-laden jets having the same injection geometry, and (2) among the different drop-laden jet geometries. All simulations were performed using n-decane as the liquid in the drops. The model and results have been documented in a manuscript that was submitted for publication [7]. The highlights of the results are described below.

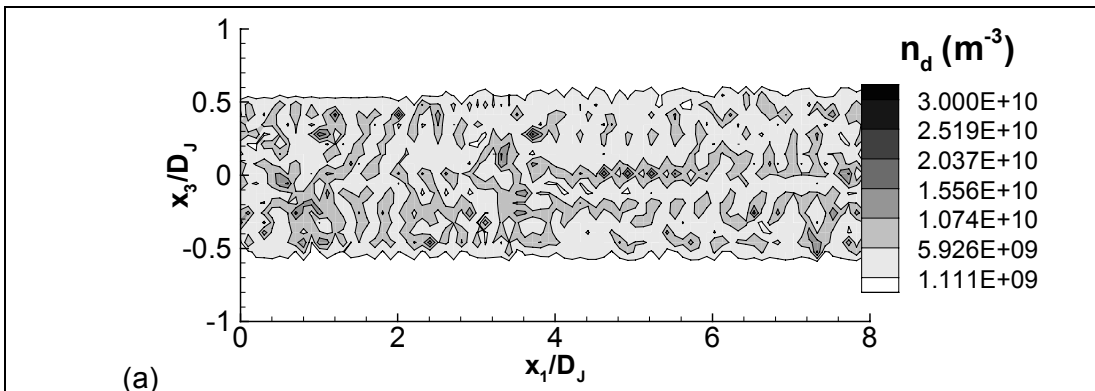
Similar to gaseous jets, two-phase flow jets with phase change were shown to reach a steady-state entrainment limit. All comparisons between simulations were performed at the time corresponding to this steady-state limit. The results showed that drop-laden gaseous jets exhibit larger entrainment than their gaseous counterpart, and that this enhancement is primarily due to the momentum interaction between drops and gas. The momentum interaction results from the combined effects of drag on the drops and of the momentum of the evaporated gas released from the drops entering the gas phase. For the present conditions, it is the drag rather than the evaporation term that contributes most to the momentum interaction. It is foreseen that the momentum interaction term will become even more important with increasing mass loading (the present simulations were all conducted with a fixed, modest, initial mass loading of 0.29).

The potential core of a jet is here defined as the region beyond which the velocity no longer equals that at the inlet, and therefore is an indicator of mixing. In 3 dimensions, this region is delineated by a surface. The potential core of non-circular gaseous jets (Fig. 4a) is shorter than that of circular jets, both in the x_1 and x_3 directions, with the square jet being closer to the circular jet and the rectangular one being the shortest; for the triangular configuration there is an asymmetry with respect to $x_3 = 0$, as expected. The result of the drop interaction with the flow (Fig. 4b) is to reduce the potential core from its single-phase value by about an order of magnitude in the streamwise direction. Moreover, it is also clear that the considerably increased streamwise vorticity detected for the two-phase jets with respect to their single-phase counterpart induces local fluctuations in the velocity (in agreement with the experimental findings of McDonell and Samuelsen [8]), typically yielding jagged and very asymmetric core profiles; however, all two-phase cores seem to be approximately of the same length (i.e. geometry-independent length for two-phase flows versus geometry-dependent length for gaseous jets).

Furthermore, none of the drop-laden jets exhibited the axis switching feature characteristic of the non-circular single-phase jets, which was attributed to the increased streamwise and spanwise vorticity in drop-laden jets.



Comparing the entrainment of drop-laden jets, the circular configuration exhibited the least entrainment, followed by the square one, while the elliptical, rectangular and triangular configuration entrained similarly. Although the triangular jet displayed the largest fine-scale production (a beneficial aspect), this occurred at the vertices and resulted in the accumulation of drops at those locations (a detrimental aspect). Combined considerations of drop-number density (Fig. 5), liquid mass (Fig. 6) and evaporated species distributions (Fig. 7) lead to recommending the elliptic jet as the optimal configuration for combining good drop and liquid-mass dispersion with good mixing characteristics.



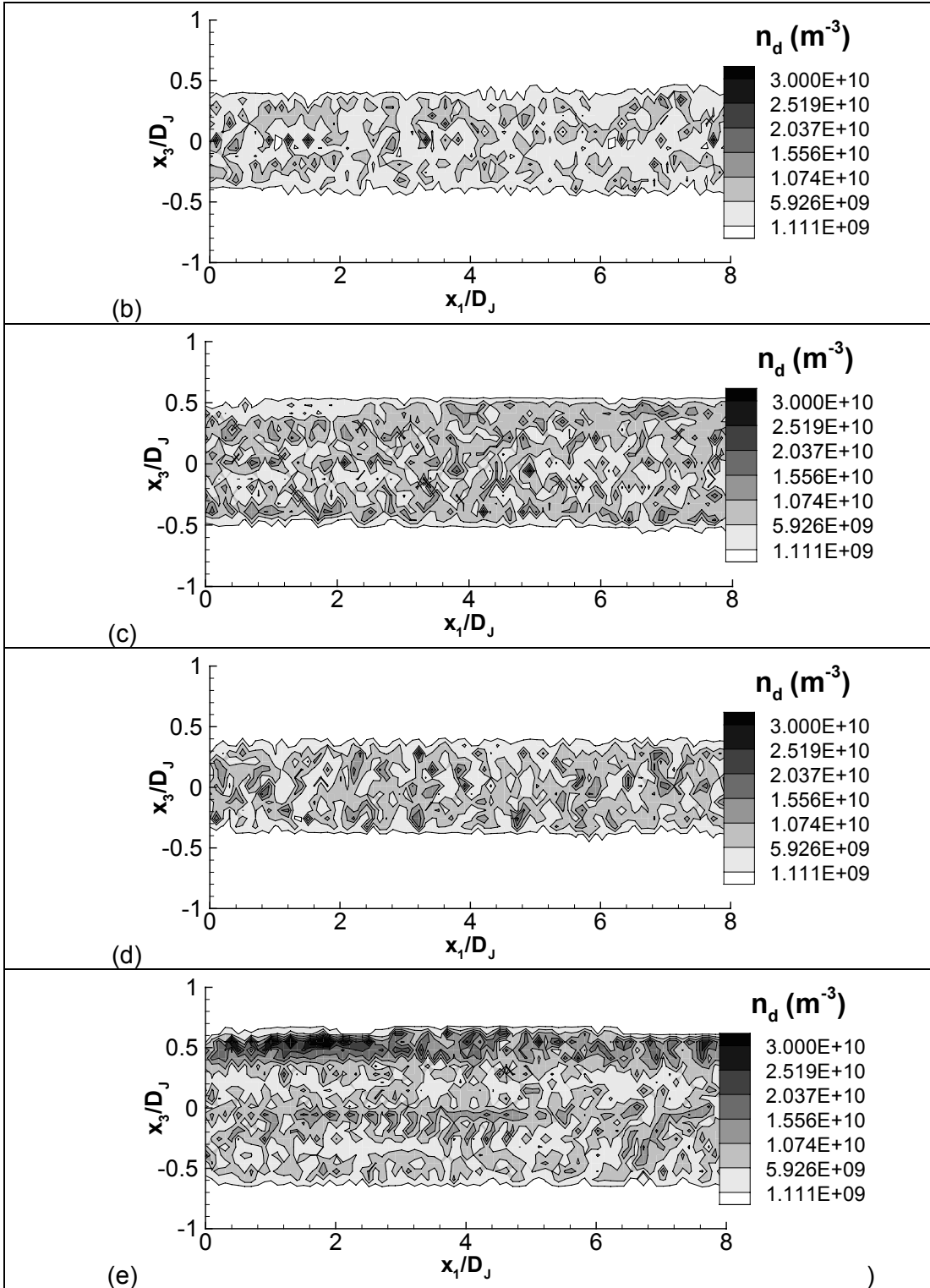
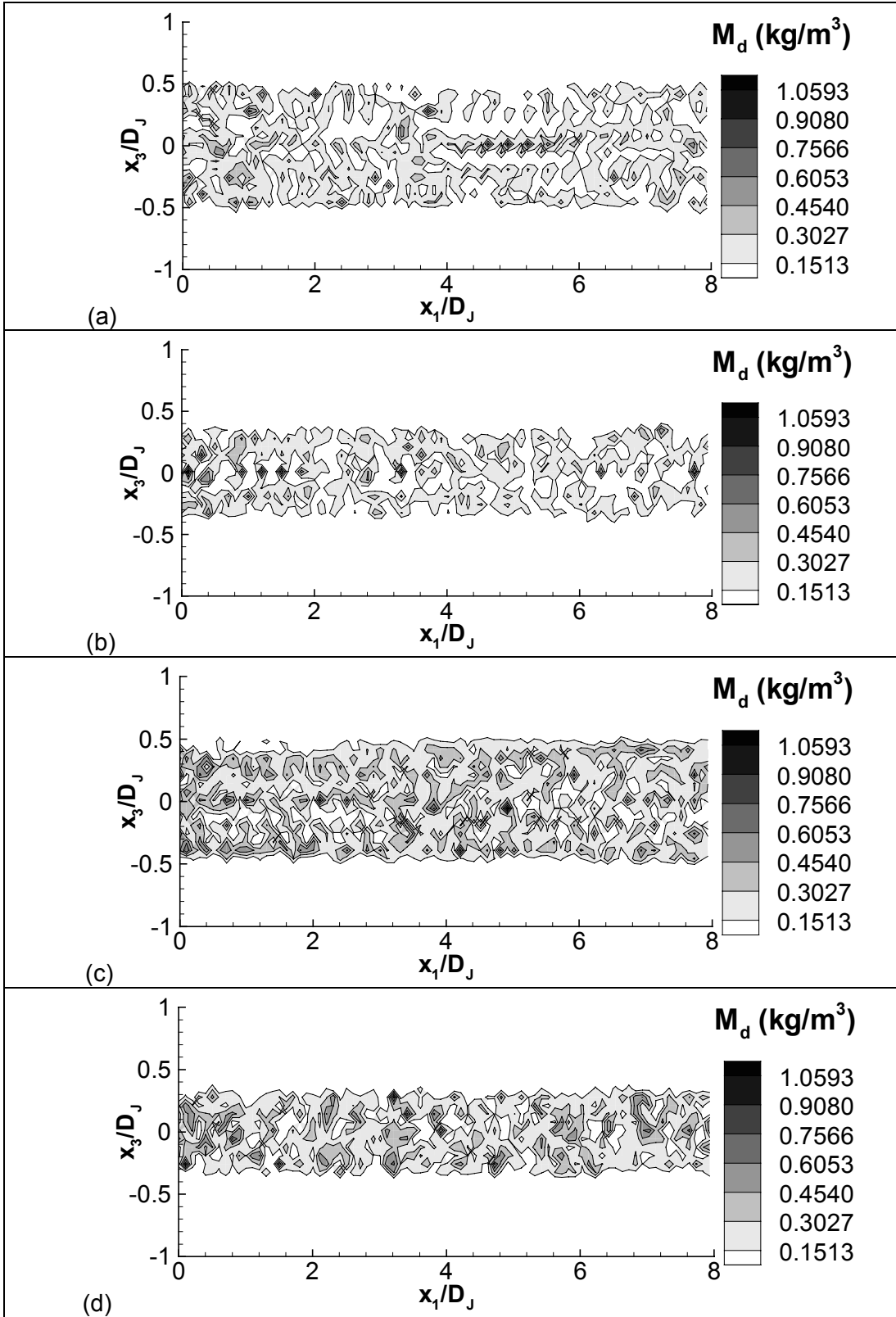


Fig. 5 Contours of instantaneous drop number density at $x_2/D_J=0$ for (a) circular jet, (b) elliptic jet, (c) square jet, (d) rectangular jet, (e) triangular jet. All at steady-state entrainment.



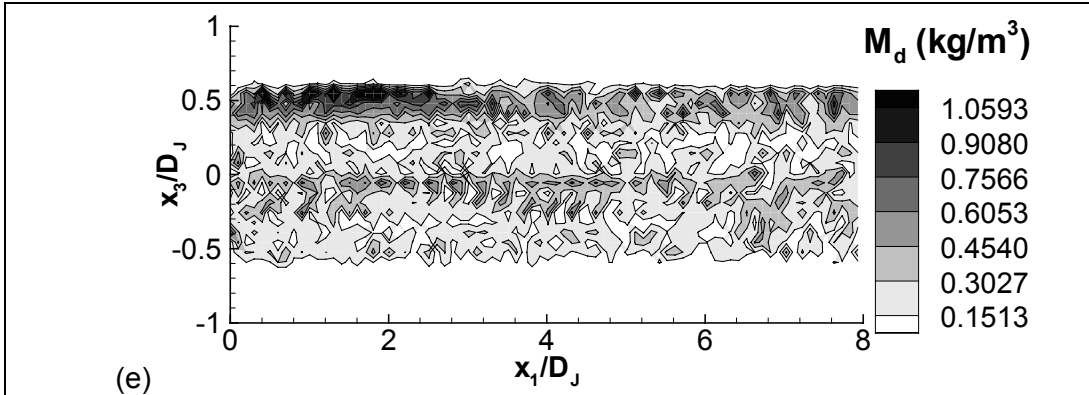
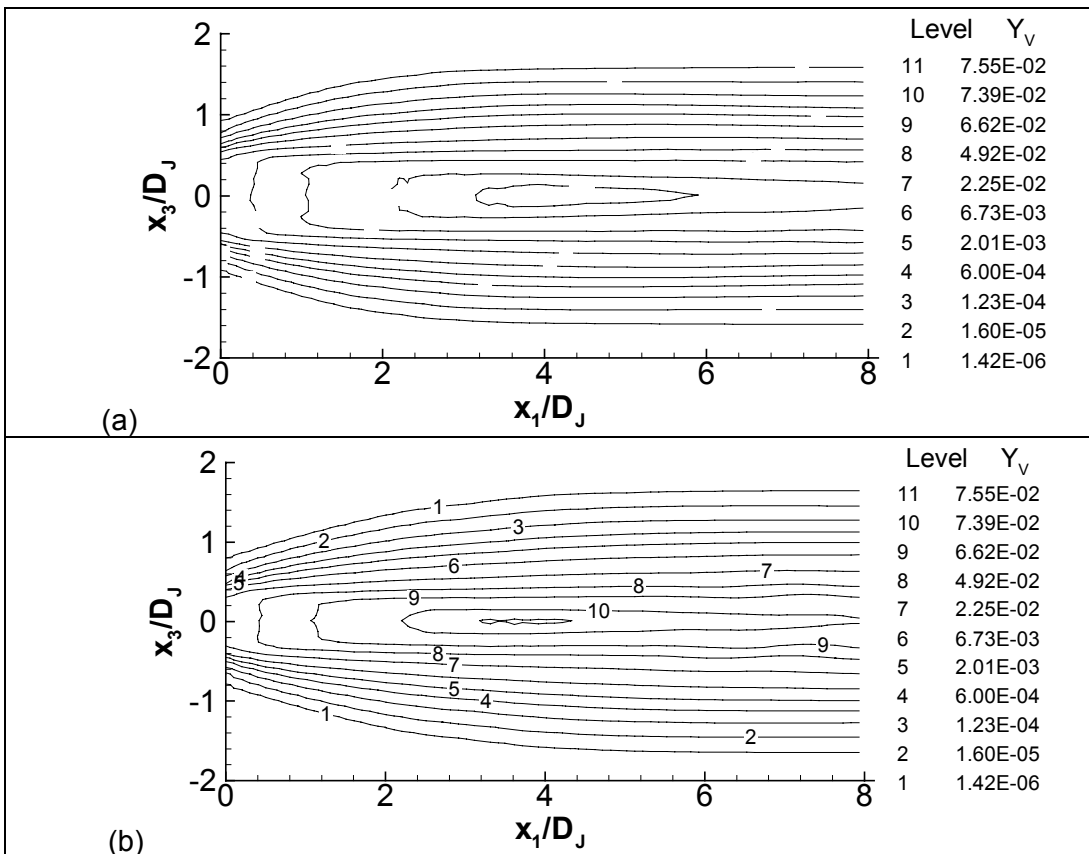
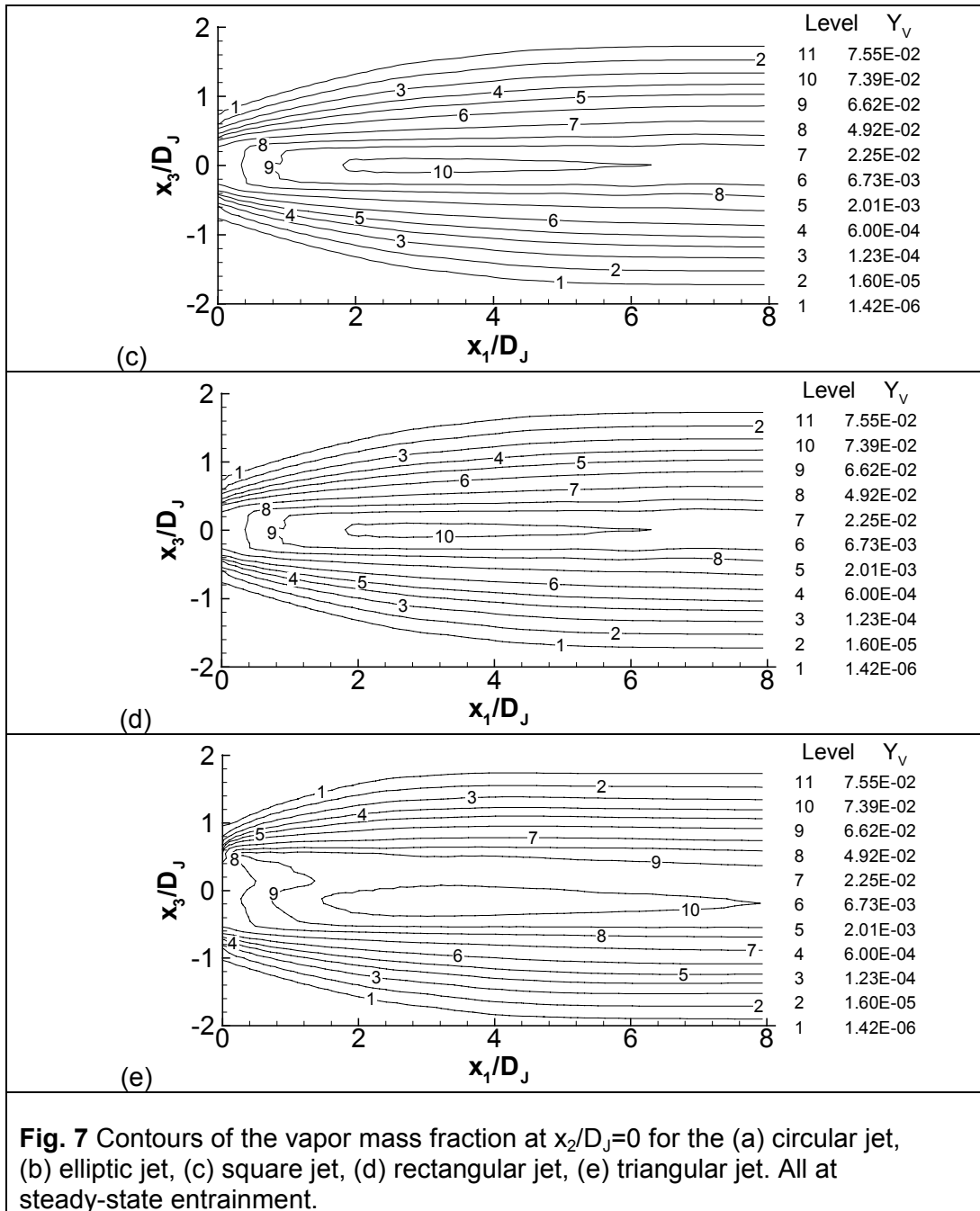


Fig. 6 Contours of instantaneous liquid mass per unit volume, at $x_2/D_J=0$ for the (a) circular jet, (b) elliptic jet, (c) square jet, (d) rectangular jet, (e) triangular jet. All at steady-state entrainment.





All these results were obtained for pre-transitional jets, and further investigations should elucidate the effect of turbulence on these findings. These future turbulent results will be obtainable once we have derived SGS models, as discussed above.

DIRECT NUMERICAL SIMULATIONS WITH MULTICOMPONENT FUEL DROPS

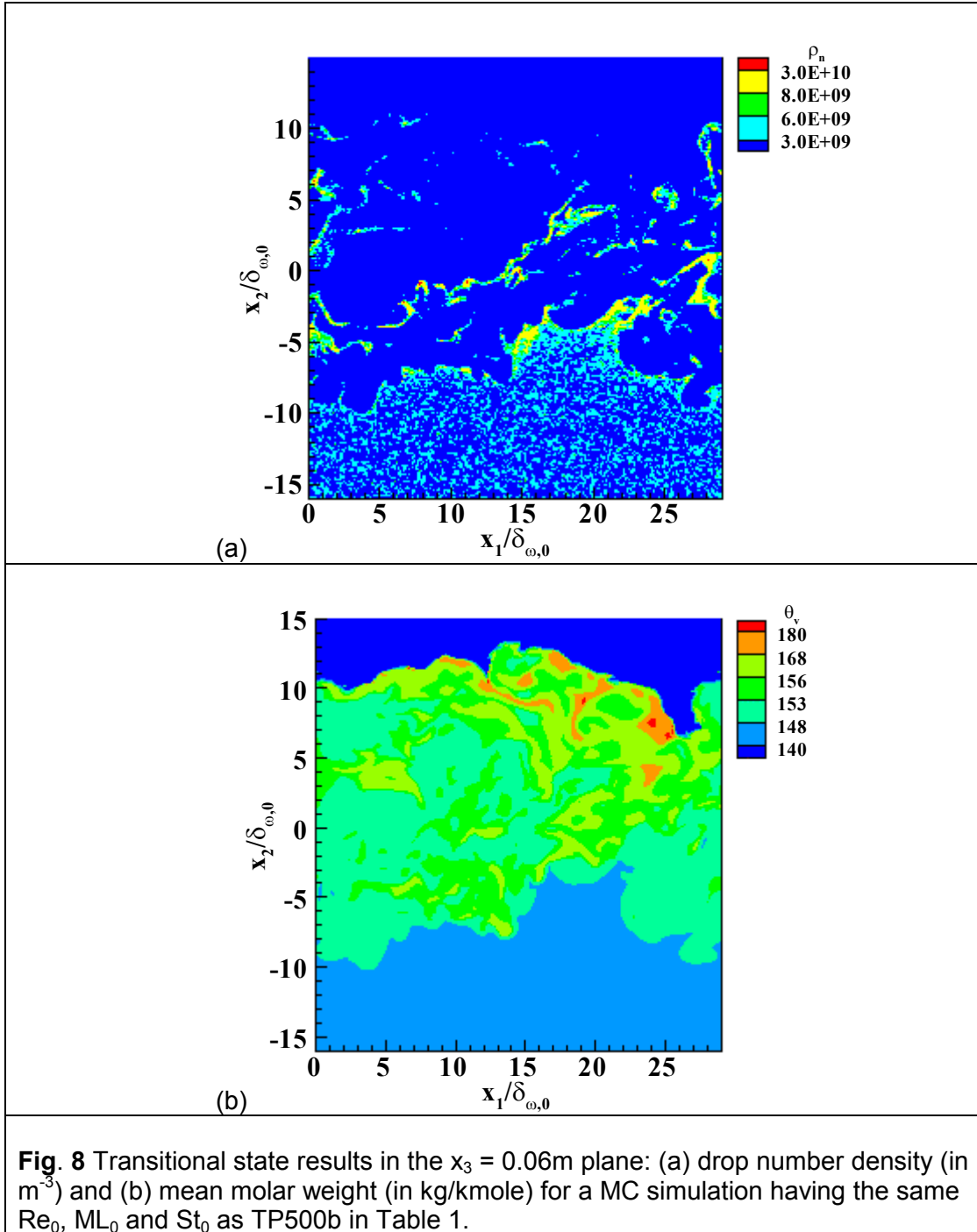
The introduction of a multicomponent (MC) fuel-drop model is motivated by the characteristics of diesel fuel, which is of primary interest in this investigation. Accounting for each individual chemical constituent of a mixture (e.g. see the single drop, binary-fuel model of [9] and the MC-

fuel drop model of [10]) may be quite impractical as a modeling approach because of computational constraints. Therefore, the strategy adopted herein is to use the statistical point of view embedded in the Continuous Thermodynamics (CT) approach. The CT approach was discussed in detail by Gal-Or et al. [11], who derived a self-consistent theory based on this concept, and by Cotterman et al. [12] in the context of phase equilibrium calculations. Based on the CT approach, Tamim and Hallett [13] and Hallett [14] have developed a model for the evaporation of a single, isolated drop of fuel that is a mixture of a multitude of species. The present study adopted the CT approach and utilized it in a study of the coupled interaction between a multitude of drops (several millions) and a flow in the context of DNS of a temporal mixing layer at atmospheric pressure.

The primary idea of CT modeling is to describe the fuel composition (both liquid and vapor) using a distribution function. Although generally the distribution function depends on many parameters representing the characteristics of the fuels, it has been shown [12] [14] that in certain cases it is possible to reduce this dependency to a single parameter: the species molar weight. This simplification is available for mixtures composed of homologous species [11] [12] and includes diesel fuel [12] [13], which is the present interest. The advantage of such a statistical description is that while a wide range of individual species can be accommodated in the mixture, the number of governing equations is minimally augmented with respect to that necessary for a single species because the composition is represented by a small number of parameters determining the distribution function.

Using these concepts, a formulation has been developed for the mixing layer (depicted in Fig. 1) laden with MC evaporating drops. DNSs with this formulation have been conducted for two purposes: (i) to compare the results of the MC simulations with those of equivalent single-component (SC) simulations to identify novelties of behavior, if any, and (ii) to characterize the important features of behavior displayed by MC situations. The model and results are described in detail in a manuscript that has been very recently submitted for publication [15]. What is presented below is only a succinct discussion of the essential results.

Similar to the SC DNS with n-decane fuel discussed above, the MC mixing layer simulations consisted of the perturbation-induced double pairing of four initial vortices to yield an ultimate vortex within which small scales proliferated. The global properties of the layers (momentum thickness, stretching and tilting effects producing small scales, and the vorticity budgets) displayed modest sensitivity to the fuel composition and the layers attained transition at similar times. Visualizations of dynamic and thermodynamic variables showed, however, that the details of the MC-fuel layers differ from their SC counterpart. MC-fuel drops evaporated slower due to the higher saturation pressure of the heavier species, leading to their interaction time with the flow being longer. This longer interaction time permitted the development of a more complex small-scale vorticity structure in the flow, and the creation of regions of higher drop number density which also displayed more structure than in the equivalent SC-fuel simulation, particularly in high strain regions. The smaller drop number density in SC cases was the combined result of SC-fuel drops becoming evaporated, and thus being removed from the computation, and of the initially smaller number of drops (ML_0 is the same in the SC and MC simulations, but the density of diesel is larger than that of n-decane). Figure 8a obtained with MC-fuel should be compared to Fig. 2 displaying the results for SC-fuel (i.e. n-decane) at otherwise same Re_0 , ML_0 and St_0 . In Fig. 8a the larger drop number density and increased structure of the drop organization (also quantitatively checked using other analytic tools) are evident.



In the SC case, the molar weight of the evaporated fuel was inherently constant and its spatial distribution followed that of the evaporated fuel mass fraction. For the MC-fuel drop case, evaporation leads to the mean molar weight in the liquid increasing and the variance initially decreasing. However, as drops were transported into regions of different gas compositions, condensation occurred, leading to an eventual increase of the liquid variance. This realistic condensation of some species coexisting with the evaporation of other species was captured with only two additional conservation equations compared to the SC-fuel situation. The slower

evaporation and the evaporation/condensation process were considered responsible for the reduced drop-size polydispersity detected in MC simulations compared to their SC counterpart. The species released from the drops contributed to increasing both the mean molar weight and the variance of the gas composition. Visualization of the mean molar weight spatial distribution in streamwise planes, shown in Fig. 8b in the $x_3=0.06\text{m}$ plane, revealed that the lighter chemical components accumulated in the lower stream as they were released early during evaporation, before the drops were entrained in the layer. Intermediary molar weight species resided in the interior of the layer because they were released after the drops were entrained and therefore participated in the mixing process resulting from the double vortex pairing. The heavier components, which were released later in the drop lifetime, resided in regions of high drop-number density. Therefore, a segregation of the chemical species occurred based on the time of their release from the drops. It is this segregation, which is important in reforming processes, that cannot be captured by the SC-fuel drop approximation. Segregation of the fuel according to molecular weight also indicates that undesirable processes, such as coking, may occur at specific locations corresponding to the high drop number density region within the flow. Since our analysis also shows that the high drop number density regions coincided with the regions of low gas vorticity and high stress, this finding may help in mitigating coking.

Further investigations of MC-fuel drop representation will focus on improving the robustness of the present model. Indeed, tests with diesel-fuel drops in a higher (than the current 375K) initial-temperature carrier gas revealed that as evaporation becomes faster the model breaks down. This indicates that the assumed invariant mathematical form of the molar-weight distribution (but with varying mean and variance) during drop evaporation is not a good assumption. A robust physical representation of the fuel composition should allow the study of a variety of fuels and in environments at higher gas temperatures than for SC fuels for which DNS results are of interest only if the gas temperature is low enough to allow survival of the drops long enough to interact with the flow. In contrast, equivalent MC-fuel drop simulations do not have this limitation and have the potential of elucidating the evolution of transitional features of the flow at different gas temperatures.

ACKNOWLEDGEMENTS

One of the authors (H. A-H) was sponsored by the Egyptian Ministry of Education through a graduate student scholarship during his stay at Caltech as a Special Graduate Student, covering the entire period of this investigation. Another author (P. C. LeC) was sponsored by a grant to the first author (J. B.) from the Donors of The Petroleum Research Fund administered by the American Chemical Society.

REFERENCES

- [1] N. Okong'o and J. Bellan, Irreversible entropy production in two-phase flows with phase change, ILASS 2002, Madison, Wisconsin, May 14-17, 2002
- [2] S. Pannala and S. Menon, On LEM/LES methodology for two-phase flows, AIAA99-2209, presented at the 35th AIAA/ASME/SAE/ASEE Joint Propulsion Conference, June 20-23, 1999 Los Angeles, CA
- [3] E. Gutmark, K. C. Schadow, T. P. Parr, D. M. Hanson-Parr and K. J. Wilson, Noncircular jets in combustion systems, *Experiments in Fluids*, 7, 248 (1989)
- [4] K. B. M. Q. Zaman, Axis switching and spreading of an asymmetric jet: the role of coherent structure dynamics, *J. Fluid Mech.*, 316, 1 (1996)
- [5] K. B. M. Q. Zaman, Spreading characteristics of compressible jets from nozzles of various geometries, *J. Fluid Mech.*, 383, 197 (1999)

- [6] E. Gutmark and F. F. Grinstein, Flow control with noncircular jets, *Annu. Rev. Fluid Mech.*, 31, 239 (1999)
- [7] H. Abdel-Hameed and J. Bellan, Direct Numerical Simulations of two-phase jet flows with different cross-section injection geometries, submitted to *Phys. Fluids*
- [8] V. G. McDonnell and G. S. Samuelsen, Structure of vaporizing pressure atomized sprays, *Atomization and Sprays*, 3, 321 (1993)
- [9] K. Harstad and J. Bellan, A Model of the evaporation of binary-fuel clusters of drops, *Atomization and Sprays*, 1, 367 (1991)
- [10] C. K. Law and H. K. Law, A d^2 -law for multicomponent droplets vaporization and combustion, *AIAA J.*, 20, 522 (1982)
- [11] B. Gal-Or, H. T. Cullinan, Jr and R. Galli, New thermodynamic-transport theory for systems with continuous component density distributions, *Chem. Eng. Sci.*, 30, 1085 (1975)
- [12] R. L. Cotterman, R. Bender, R. and J. M. Prausnitz, Phase equilibria for mixtures containing very many components. Development and application of continuous thermodynamics for chemical process design, *Ind. Eng. Chem. Process Des. Dev.*, 24, 194 (1985)
- [13] J. Tamim and W. L. H. Hallett, A continuous thermodynamics model for multicomponent droplet vaporization, *Chem. Eng. Sci.*, 50, 2933 (1995)
- [14] W. L. H. Hallett, A simple model for the vaporization of droplets with large numbers of components, *Combustion and Flame*, 121, 334 (2000)
- [15] P. C. Le Clercq and J. Bellan, Direct numerical simulation of a transitional temporal mixing layer laden with multicomponent-fuel evaporating drops using continuous thermodynamics, submitted to the *J. Fluid Mech.*